

1-1-2016

Wavefront-ray grid FDTD algorithm

MEHMET ÇİYDEM

Follow this and additional works at: <https://journals.tubitak.gov.tr/elektrik>



Part of the [Computer Engineering Commons](#), [Computer Sciences Commons](#), and the [Electrical and Computer Engineering Commons](#)

Recommended Citation

ÇİYDEM, MEHMET (2016) "Wavefront-ray grid FDTD algorithm," *Turkish Journal of Electrical Engineering and Computer Sciences*: Vol. 24: No. 3, Article 13. <https://doi.org/10.3906/elk-1309-240>
Available at: <https://journals.tubitak.gov.tr/elektrik/vol24/iss3/13>

This Article is brought to you for free and open access by TÜBİTAK Academic Journals. It has been accepted for inclusion in Turkish Journal of Electrical Engineering and Computer Sciences by an authorized editor of TÜBİTAK Academic Journals. For more information, please contact academic.publications@tubitak.gov.tr.

Wavefront-ray grid FDTD algorithm

Mehmet ÇİYDEM^{1,*}, Sencer KOÇ²

¹Engitek Ltd., Balgat, Ankara, Turkey

²Department of Electrical and Electronics Engineering, Faculty of Engineering, Middle East Technical University, Ankara, Turkey

Received: 30.09.2013

Accepted/Published Online: 18.12.2013

Final Version: 23.03.2016

Abstract: A finite difference time domain algorithm on a wavefront-ray grid (WRG-FDTD) is proposed in this study to reduce numerical dispersion of conventional FDTD methods. A FDTD algorithm conforming to a wavefront-ray grid can be useful to take into account anisotropy effects of numerical grids since it features directional energy flow along the rays. An explicit and second-order accurate WRG-FDTD algorithm is provided in generalized curvilinear coordinates for an inhomogeneous isotropic medium. Numerical simulations for a vertical electrical dipole have been conducted to demonstrate the benefits of the proposed method. Results have been compared with those of the spherical FDTD algorithm and it is showed that numerical grid anisotropy can be reduced highly by WRG-FDTD.

Key words: Finite difference time domain, wavefront, ray, numerical dispersion, grid anisotropy, directional propagation

1. Introduction

The conventional finite difference time domain (FDTD) algorithm proposed by Yee [1] has been the milestone to solve time-dependent Maxwell's curl equations directly on numerical space grids with time updates. It is an explicit, second-order accurate algorithm in time and space. Since then, extensions of this algorithm to various gridding structures, reduction of numerical dispersion, and mitigation of stability condition have been done continuously [2].

As for gridding of the medium and scattering objects, the conventional FDTD has been restricted to rectangular grids and has some problems in modeling the curved surfaces/boundaries of objects accurately. A general remedy has been to apply a staircasing method to the curved surfaces with very fine grids to have better representation and accurate results. However, decreasing the cell size does not always give predictable improvements and one may need subpixel smoothing schemes further to minimize errors [3], which requires modification of the real boundary conditions and use of an anisotropic technique. In 1983, Holland [4], based on the work of Stratton [5], developed a FDTD algorithm for generalized curvilinear coordinates. Fusco and Fusco et al. [6,7] revisited and extended Holland's formulation. Generalization of this approach assuming local curvilinear coordinates for cell faces was achieved by Lee et al. [8]. In this respect, a number of alternate FDTD methods have also been proposed, such as the contour path FDTD [9], discrete surface integral FDTD [10], and nonorthogonal FDTD [11], in generalized curvilinear coordinates by using conformal meshes instead of staircasing for curved surfaces.

Discretization of partial differential equations and gridding inherently causes numerical dispersion, which

*Correspondence: mehmet.ciydem@engitek.com.tr

makes any FDTD method difficult to apply to large-scale and phase-sensitive problems. The above methods pay attention to reducing numerical dispersion in some respects but not generating a specific grid for dispersion. In this paper, rather than proposing a new FDTD method for curved surfaces/boundaries, a conformal FDTD algorithm that conforms to the wavefront-ray grid (WRG-FDTD) is proposed for wave propagation. We claim that the wavefront-ray grid will reduce numerical dispersion by taking into account directional energy propagation. A simple, second-order accurate, explicit WRG-FDTD algorithm has been developed and simulations have been conducted for an inhomogeneous isotropic medium for a vertical electrical dipole (VED).

2. FDTD numerical dispersion and grid structure

In all FDTD methods, the computational domain grid is generated either arbitrarily and/or conforming to the curved surfaces of object. Although this grid generation is mathematically valid, the physical waves propagating in the grid are ignorant of this grid structure, so they experience different numerical phase velocities and grid anisotropy. Numerical dispersion inherent to FDTD mainly stems from these two unphysical errors. Dispersive errors build up linearly with distance and establish the basic limitation to every grid-based Maxwell solver. To mitigate this limitation, modifications to the conventional FDTD algorithm, such as centering the numerical phase velocity or use of higher order spatial differences, led to new low dispersion algorithms including MRTD by Krumpholz and Katehi [12], PSTD by Liu [13], the angle optimized algorithm by Wang and Teixeira [14], and the higher order FDTD method by Zygridis and Tsiboukis [15]. Other low numerical dispersion and anisotropy FDTD algorithms [16,17] have also been reported.

In a uniform Cartesian FDTD grid, the following 3D numerical dispersion relation (NDR) holds:

$$\left[\frac{1}{v_p \Delta t} \sin \left(\frac{\omega \Delta t}{2} \right) \right]^2 = \left[\frac{1}{\Delta x} \sin \left(\frac{k_x^* \Delta x}{2} \right) \right]^2 + \left[\frac{1}{\Delta y} \sin \left(\frac{k_y^* \Delta y}{2} \right) \right]^2 + \left[\frac{1}{\Delta z} \sin \left(\frac{k_z^* \Delta z}{2} \right) \right]^2, \quad (1)$$

where $k^* = k_x^* \hat{x} + k_y^* \hat{y} + k_z^* \hat{z}$ and v_p are numerical wave number vector and phase velocity, respectively. Liu [18] analyzed the conventional FDTD grid and alternative grids for numerical dispersion. Qualitatively speaking, numerical dispersion errors can be reduced to any desired level by employing sufficiently fine gridding ($\Delta x \rightarrow 0$, $\Delta y \rightarrow 0$, $\Delta z \rightarrow 0$) and the theoretical ideal dispersion relation $k = \omega/v_p$ is obtained. Numerical dispersion can also be made optimal if the Courant–Friedrich–Levy stability number and direction of propagation are chosen suitably (equality case of stability condition and diagonal propagation). However, for general 2D/3D electromagnetic problems, all these have little practical use.

In generalized curvilinear coordinates, the NDR expression cannot be formulated neatly as in Eq. (1). Navarro et al. [19] and Ray [20] studied the stability and numerical dispersion aspects of algorithms for conformal grids. Numerical dispersion, which is studied with variations in numerical phase velocity Δv_{phy} and grid anisotropy Δv_{aniso} , was also quantitatively discussed in [21] with nonorthogonal meshes only for some uniform skewed cases. Δv_{aniso} is useful in quantifying wavefront distortion. Numerical waves in 2D/3D grids exhibit nonphysical variation of phase velocity as a function of numerical wave vector k^* . Thus, the grid behaves like an anisotropic medium. The nature of gridding determines this anisotropy Δv_{aniso} in a manner that is almost independent of time stepping Δt . A suitable choice of time discretization can improve total numerical dispersive error by reducing Δv_{phy} , but it cannot reduce the anisotropy Δv_{aniso} resulting from spatial gridding.

The proposed FDTD algorithm on a wavefront-ray grid structure has been put forward [22] to reduce grid anisotropy Δv_{aniso} of FDTD numerical dispersion because this special grid structure, by its nature, is

aligned with actual wave propagation vector ($k = k_x \hat{x} + k_y \hat{y} + k_z \hat{z}$), which is in the direction of energy flow, Poynting vector ($E \times H$). To the best of the authors' knowledge, conformal gridding in this sense has not been proposed before. Formulation and implementation of WRG-FDTD has been introduced and it is shown that grid anisotropy Δv_{aniso} can be eliminated by WRG-FDTD.

3. WRG-FDTD formulation and implementation

The gist of the proposed method relies on the special grid structure and computations done on it [22]. Grids are generated so that they lie on the wavefront surfaces and along the ray trajectories. Before starting computations, the initial wavefront on which sources/fields are defined is meshed for desired resolution and accuracy. Moving in the ray direction ($E \times H$) by an amount Δt , which is determined by the stability condition, the new grid points on the next wavefront are constructed. The grid generation procedure is continued in this way until the entire grid is created in generalized curvilinear coordinates by using medium parameters (ϵ, μ).

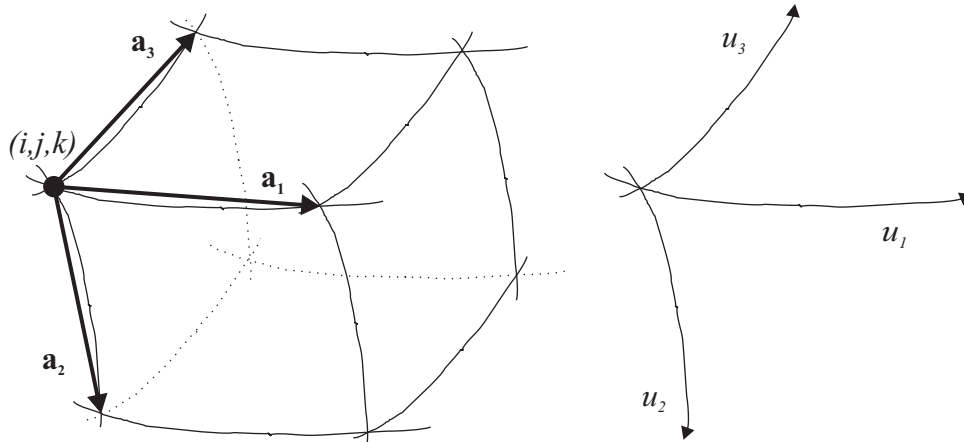


Figure 1. General curvilinear system and a typical cell.

Mathematically, the grid cell in the computational domain is approximated as a parallelepiped whose sides are the basis vectors (a_1, a_2, a_3). Reciprocal basis vectors (b_1, b_2, b_3) are defined as:

$$b_1 = \frac{a_2 \times a_3}{V}, b_2 = \frac{a_3 \times a_1}{V}, b_3 = \frac{a_1 \times a_2}{V}. \tag{2}$$

$V = a_1 \cdot (a_2 \times a_3)$ is the volume of the cell. The metric and inverse metric tensors also have the following elements respectively:

$$g_{ij} = a_i \cdot a_j, h_{ij} = b_i \cdot b_j. \tag{3}$$

(a_i, a_j) and (b_i, b_j) satisfy $\delta_{ij} = a_i \cdot a_j$ and $\delta_{ij} = b_i \cdot b_j$ where δ_{ij} is the Kronecker delta. Any vector field in generalized curvilinear coordinates can be written in terms of basis and reciprocal basis vectors [5]. For example, electric field E can be expanded as:

$$E = \sum_{i=1}^3 E_{b_i} a_i = \sum_{i=1}^3 E_{a_i} b_i, \tag{4}$$

where $E_{a_i} = E \cdot a_i, E_{b_i} = E \cdot b_i$ are called covariant and contravariant components of E and can be written in terms of each other as follows:

$$E_{a_i} = \sum_{j=1}^3 g_{ij} E_{b_j}, E_{b_i} = \sum_{j=1}^3 h_{ij} E_{a_j}. \tag{5}$$

With the above generalized curvilinear coordinates' preliminary, discretization of Maxwell's curl equations leads to the following update equations in terms of covariant and contravariant components of \mathbf{E} and \mathbf{H} similar to S-FDTD [23]. Note that these update equations are two-dimensional since the sample VED radiation problem is symmetric around the ϕ -axis and can be treated as a 2D problem in θ and r variables.

$$\begin{aligned} E_{b_1}^{n+1}(i, k) &= E_{b_1}^n(i, k) + \frac{\Delta t}{\varepsilon_0 \varepsilon_r(i, k) V(i, j, k)} \left\{ H_{a_3}^{n+1/2}(i, k) - H_{a_3}^{n+1/2}(i, k - 1) \right\} \\ E_{b_2}^{n+1}(i, k) &= E_{b_2}^n(i, k) + \frac{\Delta t}{\varepsilon_0 \varepsilon_r(i, k) V(i, j, k)} \left\{ H_{a_3}^{n+1/2}(i, k) - H_{a_3}^{n+1/2}(i - 1, k) \right\} \\ H_{b_3}^{n+1/2}(i, k) &= H_{b_3}^{n-1/2}(i, k) + \frac{\Delta t}{\mu_0 V(i, j, k)} \left\{ \begin{aligned} &E_{a_2}^n(i + 1, k) - E_{a_2}^n(i, k) \\ &+ E_{a_1}^n(i, k + 1) - E_{a_2}^n(i, k) \end{aligned} \right\} \end{aligned} \tag{6}$$

4. Sample problem and numerical studies

It is conjectured that the VED radiation problem in the isotropic, inhomogeneous medium shown in Figure 2 can be solved. For simulation, as an initial condition, an electric field is defined on an initial wavefront whose radius $r_0 = 1m$ is centered at the origin. Inhomogeneity is introduced along the z -axis, and then the azimuth ϕ -axis symmetry can still be utilized and all works can be done only on the yz -plane as a 2D problem. Medium inhomogeneity is as follows:

$$\varepsilon_r(z) = \begin{cases} 1 & \text{elsewhere} \\ 1 - (z + 10)/5 & z \leq -10 \end{cases} \tag{7}$$

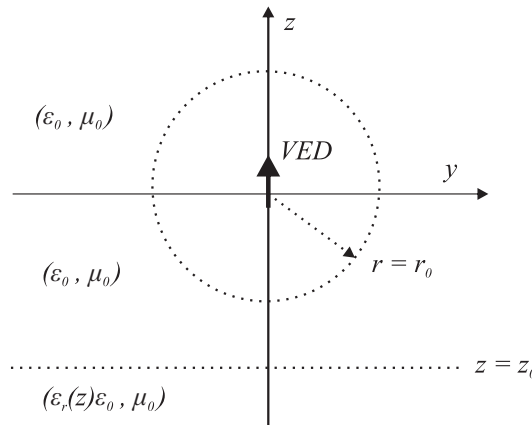


Figure 2. VED radiation problem.

Examples of grid generation along the rays are given in Figures 3 and 4, which illustrate ray trajectories and wavefronts for coarse (minimum spatial spacing $\leq \lambda_{\min}/5$) and fine gridding (minimum spatial spacing $\leq \lambda_{\min}/10$).

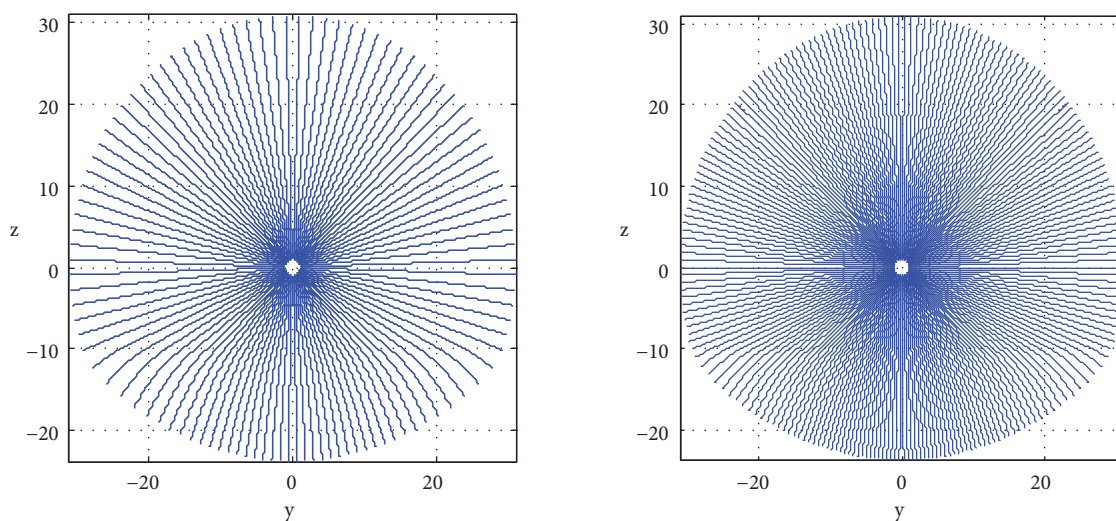


Figure 3. Rays for coarse and fine gridding.

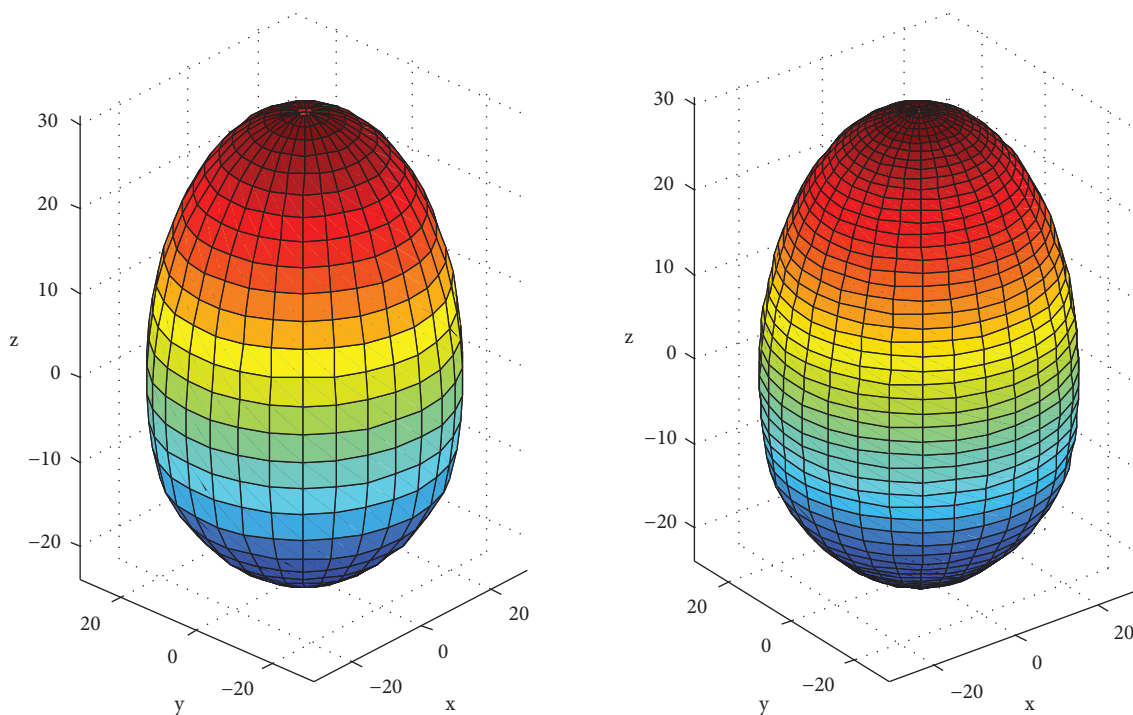


Figure 4. Wavefronts for coarse and fine gridding.

Analytical ray trajectories for given permittivity profile can be obtained by:

$$y(z) = \int_{z_0}^z \frac{ad\gamma}{\sqrt{n^2(\gamma) - a^2}} \tag{8}$$

Examples of analytical rays from Eq. (8) and numerical rays with launching angles ($\theta = 107^\circ, 122^\circ, 143^\circ, 162^\circ, 170^\circ$) starting on the initial wavefront and moving in the direction of energy flow as described in Section

3 are depicted in Figure 5. They are in very close agreement (overlapped) even for coarse gridding; hence, we can rely on generated grid points on the rays and our computations in this grid.

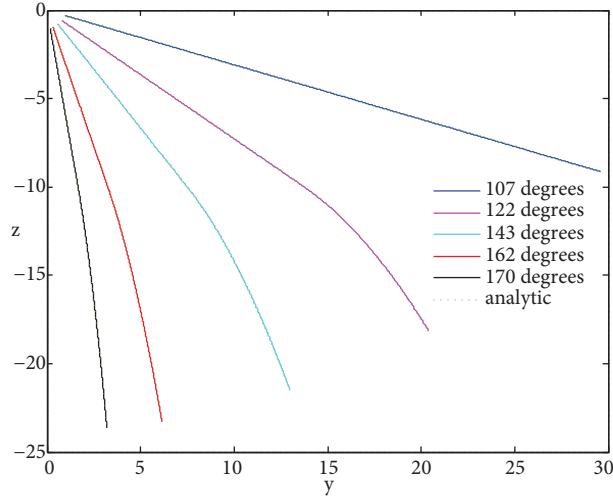


Figure 5. Analytical and numerical ray trajectories for computational grid (coarse case).

For simulations, Gaussian excitation is assumed at the VED source. For the proposed WRG-FDTD for the problem under consideration, computations have been performed based on update equations in Eq. (6) and they yielded the following results for each ray ($\theta = 107^\circ, 122^\circ, 143^\circ, 162^\circ, 170^\circ$) for both coarse and fine grids (Figures 6–9). The S-FDTD of [23] is used for comparison with WRG-FDTD. The $E_\theta = E_{th}$ component propagated along rays (Figure 5) into the inhomogeneous region is calculated. Note that S-FDTD is expected to yield good results due to the problem of spherical geometry. However, it is still ignorant of the nature of wave propagation. Hence, instead of S-FDTD, if rectangular FDTD were used, results would be worse. WRG-FDTD performs much better than even S-FDTD. Waveform distortions (Δv_{aniso}) due to phase errors caused by numerical dispersion have almost been removed.

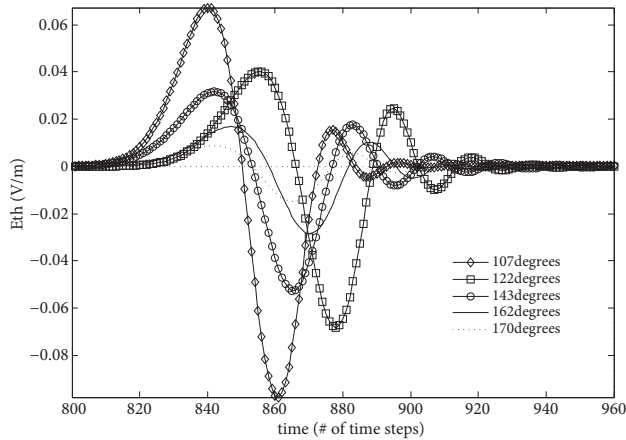


Figure 6. S-FDTD for coarse grid.

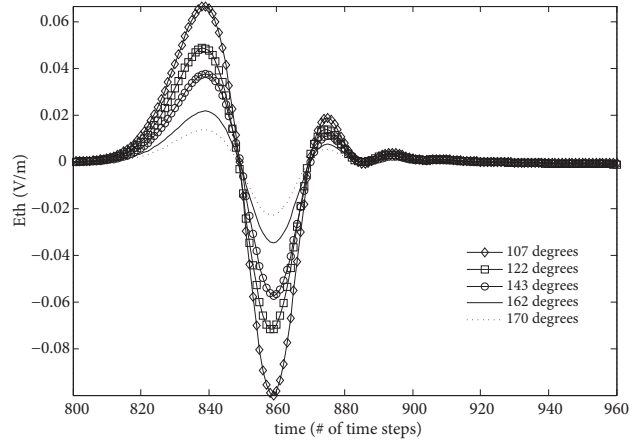


Figure 7. WRG-FDTD for coarse grid.

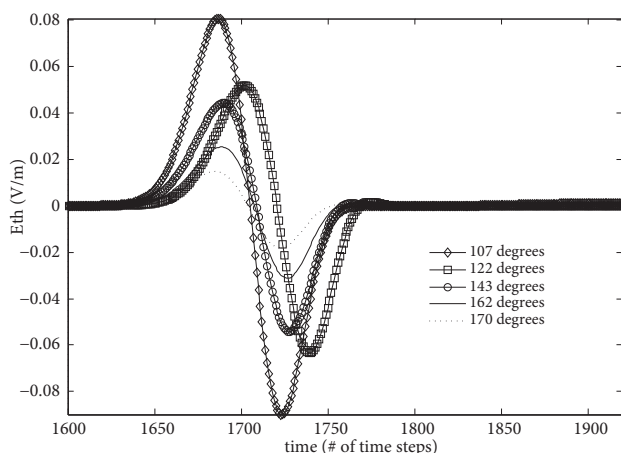


Figure 8. S-FDTD for fine grid.

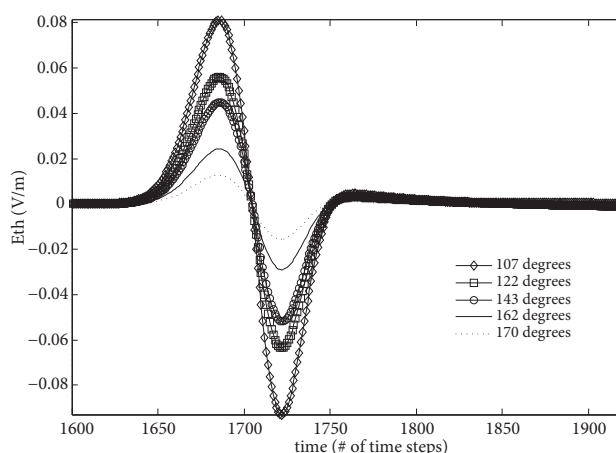


Figure 9. WRG-FDTD for fine grid.

5. Conclusions

A FDTD algorithm (WRG-FDTD) whose computational grid conforms to wavefronts and rays in the medium is presented in this paper to reduce numerical dispersion inherent to FDTD methods. A second-order accurate, explicit, and simple formulation is provided in generalized curvilinear coordinates for an inhomogeneous, isotropic medium. It takes into account directional energy flow along the rays and hence removes the anisotropy Δv_{aniso} of the conventional FDTD grid, even with S-FDTD ideal for VED problem geometry. Quantitatively it is observed that the Δv_{aniso} effect on numerical dispersion is eliminated. Numerical wave modes on each ray still experience the same type and amount of Δv_{phy} on numerical dispersion but no Δv_{aniso} directional dependence. The proposed WRG-FDTD is an explicit algorithm and its stability analysis in generalized curvilinear coordinates has already been covered in [19,20]. As mentioned before, exact numerical dispersion analysis in generalized curvilinear coordinates is not available yet but [21] tried to quantify it only for some skewed angles.

Compared to conventional FDTD grids, the use of WRG-FDTD brings some complications in generation of high-fidelity grids because a unique grid (WRG) for each problem must be generated before starting computations. However, WRG-FDTD appears very useful for eliminating Δv_{aniso} of numerical dispersion for phase sensitive, high accuracy, electrically large problems. Luckily, very good grid generation software from ray tracing is available today. Future studies will cover more complex electromagnetic problems such as reflection, refraction, and possibly diffraction for single/multiple sources and scatterers.

References

- [1] Yee KS. Numerical solution of initial boundary value problems involving Maxwell's equations in isotropic media. IEEE T Antenn Propag 1966; 14: 302-307.
- [2] Taflove A, Hagness SC. Computational Electrodynamics–The Finite Difference Time Domain Method. 3rd ed. Boston, MA, USA: Artech House, 2005.
- [3] Farjadpour A, Roundy D, Rodriguez A, Ibanescu M, Bermel P, Joannopoulos JD, Johnson SG, Burr GW. Improving accuracy by subpixel smoothing in the finite-difference time domain. Opt Lett 2006; 31: 2972-2974.
- [4] Holland R. Finite difference solution of Maxwell's equations in generalized non-orthogonal coordinates. IEEE T Nucl Sci 1983; 30: 4589-4591.

- [5] Stratton JA. *Electromagnetic Theory*. New York, NY, USA; McGraw-Hill, 1941.
- [6] Fusco M. FDTD algorithm in curvilinear coordinates. *IEEE T Antenn Propag* 1990; 38: 76-89.
- [7] Fusco M, Smith MV, Gordon LW. Three-dimensional FDTD algorithm in curvilinear coordinates. *IEEE T Antenn Propag* 1991; 39: 1463-1471.
- [8] Lee JF, Palandech R, Mittra R. Modeling three-dimensional discontinuities in waveguides using nonorthogonal FDTD algorithm. *IEEE T Microw Theory* 1992; 40: 346-352.
- [9] Jurgens TG, Taflove A, Umashankar KR, Moore TG. Finite difference time domain modelling of curved surfaces. *IEEE T Antenn Propag* 1992; 40: 357-366.
- [10] Hao Y, Railton CJ. Analyzing electromagnetic structures with curved boundaries on Cartesian FDTD meshes. *IEEE T Microw Theory* 1998; 46: 82-88.
- [11] Gedney S, Lansing FS, Rascode DL. Full wave analysis of microwave monolithic circuit devices using a generalized Yee algorithm based on an unstructured grid. *IEEE T Microw Theory* 1996; 44: 1393-1400.
- [12] Krumpholz M, Katehi LPB. MRTD: New time domain schemes based on multiresolution analysis. *IEEE T Microw Theory* 1997; 45: 385-393.
- [13] Liu QH. The PSTD algorithm: a time domain method requiring only two cells per wavelength. *Microw Opt Technol Lett* 1997; 1: 158-165.
- [14] Wang S, Teixeira FL. A three-dimensional angle-optimized finite difference time domain algorithm. *IEEE T Microw Theory* 2003; 51: 811-817.
- [15] Zygridis TT, Tsiboukis TD. Development of higher order FDTD schemes with controlled dispersion error. *IEEE T Antenn Propag* 2005; 53: 2952-2960.
- [16] Zhang XQ, Nie ZP, Xia MY, Qu SW, Li YH. Novel FDTD method with low numerical dispersion and anisotropy. In: *PIERS Proceedings*; 20–23 March 2011; Marrakesh, Morocco. pp. 718-721.
- [17] Kong Y, Chu Q, Li R. Two efficient unconditionally stable four stages split step FDTD methods with low numerical dispersion. *PIER B* 2013; 48: 1-22.
- [18] Liu Y. Fourier analysis of numerical algorithms for the Maxwell equations. *J Comput Phys* 1996; 124: 396-416.
- [19] Navarro EA, Wu C, Chung PY, Litva J. Some considerations about the finite difference time domain method in general curvilinear coordinates. *IEEE Microw Guided W* 1994; 4: 396-398.
- [20] Ray SL. Numerical dispersion and stability characteristics of time-domain methods on nonorthogonal meshes. *IEEE T Antenn Propag* 1993; 41: 233-235.
- [21] Nilavalan R, Craddock IJ, Railton CJ. Quantifying numerical dispersion in non-orthogonal FDTD meshes. *IEE P-Microw Anten P* 2002; 149: 23-27.
- [22] Ciydem M, Koc S. FDTD algorithm on wavefront-ray grid for wave propagation. In: *IEEE APS/URSI Symposium*; July 2006; Albuquerque, NM, USA. pp. 3821-3824.
- [23] Holland R. THREDS: A finite-difference time-domain EMP code in 3D spherical coordinates. *IEEE T Nucl Sci* 1983; 3: 4592-4595.